ACS OMEGA

Open Access

http://pubs.acs.org/journal/acsodf

Article

Tuning a Superhydrophobic Surface on an Electrospun Polyacrylonitrile Nanofiber Membrane by Polysulfone Blending

Rizky Aflaha, Linda Ardita Putri, Chlara Naren Maharani, Aditya Rianjanu, Roto Roto, Hutomo Suryo Wasisto, and Kuwat Triyana*

Cite This: *ACS Omega* 2024, 9, 29840−29847

Read Online

ACCESS | Metrics & More | Article Recommendations

ABSTRACT: Nanofibers made of different materials have been continuously studied and widely used as membranes due to their simple fabrication techniques and tunable surface characteristics. In this work, we developed polyacrylonitrile (PAN) nanofiber membranes by the electrospinning method and blended them with polysulfone (PSU) to obtain superhydrophobic surfaces on the fiber structures. The scanning electron microscopy (SEM) images show that the fabricated nanofibers have smooth and continuous morphology. In addition, to observe the effect of the PSU-based blending material, Fourier-transform infrared (FTIR) spectra of the samples were acquired, providing chemical compositions of the bare and PSU-blended PAN nanofibers. The fabricated PSU/PAN composite nanofibers have a diameter range of 222−392 nm. In terms of the wettability, the measured water contact angle (WCA) value of the PAN nanofibers was improved from (14 ± 1)° to (156 ± 6)°, (160 ± 4)°, (156 ± 6)°, and (158 ± 4)° after being blended with PSU solutions having concentrations of 0.5, 1, 1.5, and 2 wt %, respectively. This result has proven that the PAN nanofiber surfaces can be tuned from hydrophilic to superhydrophobic characteristics simply by introducing PSU into the PAN solution prior to electrospinning, where a small PSU concentration of 0.5% has been sufficient to provide the desired effect. Owing to its low-cost and highly efficient process, this strategy may be further explored for other types of polymer-based nanofibers.

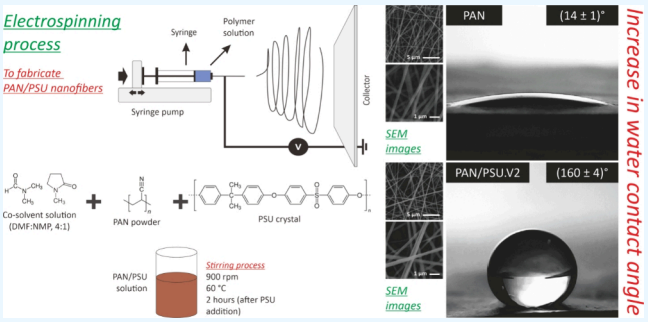

INTRODUCTION

Nanofibers have been widely used in several applications that positively affect human life (e.g., in wound dressing,[1,2] energy storage,[3,4] humidity and gas sensors,[5−11] drug delivery,[12] water filtration,[13] and air filtration[14,15]). In the case of nanofibers used for air filtration, they demonstrate superior properties, such as high mechanical strength, good air permeability, ease of modifying properties, and high filtration efficiency.[16,17] The air filtration efficiency level of nanofiber-based membranes depends on several factors. One of the most important aspects that can influence this efficiency level is their surface hydrophobicity.[18−20] A highly hydrophobic membrane, which usually comes from nonpolar material, is desired because it can repel water. Hence, the condition of the membrane can be kept dry, and its air filtration performance can be maintained at a high efficiency level with a longer operating lifetime.

To create nanofiber-based membranes, various fabrication methods can be applied, by either electrospinning or nonelectrospinning techniques (e.g., interfacial polymerization, drawing, spinneret-based tunable engineered parameters, template synthesis, phase separation, self-assembly, and freeze-drying).[21] Electrospinning, however, has become the most favorable nanofiber fabrication method because of its simple process, low-cost instrument, easy parameter adjustment, and scalable manufacturing in the industry.[6−8,22−24] Furthermore, to yield smooth and continuous nanofibers, the selection and preparation of the polymers as a base material should be carried out carefully because their electrospinnability strongly relies on the opted polymer characteristics. Here, polymer molecular weight, which reflects the entanglement number of polymer chains in solution, has become one of the most important factors affecting solution viscosity. Thus, low molecular weight polymers (e.g., poly(4-vinylpyridine) (P4VP)) are not desirable to be used because they often result in fibers with bead structures.[25]

Among the polymers that can be built as nanofibers by means of electrospinning, polyacrylonitrile (PAN) has been a popular base material due to its high molecular weight, excellent mechanical strength, good thermal resistance,

Received: April 12, 2024
Revised: June 8, 2024
Accepted: June 11, 2024
Published: June 27, 2024

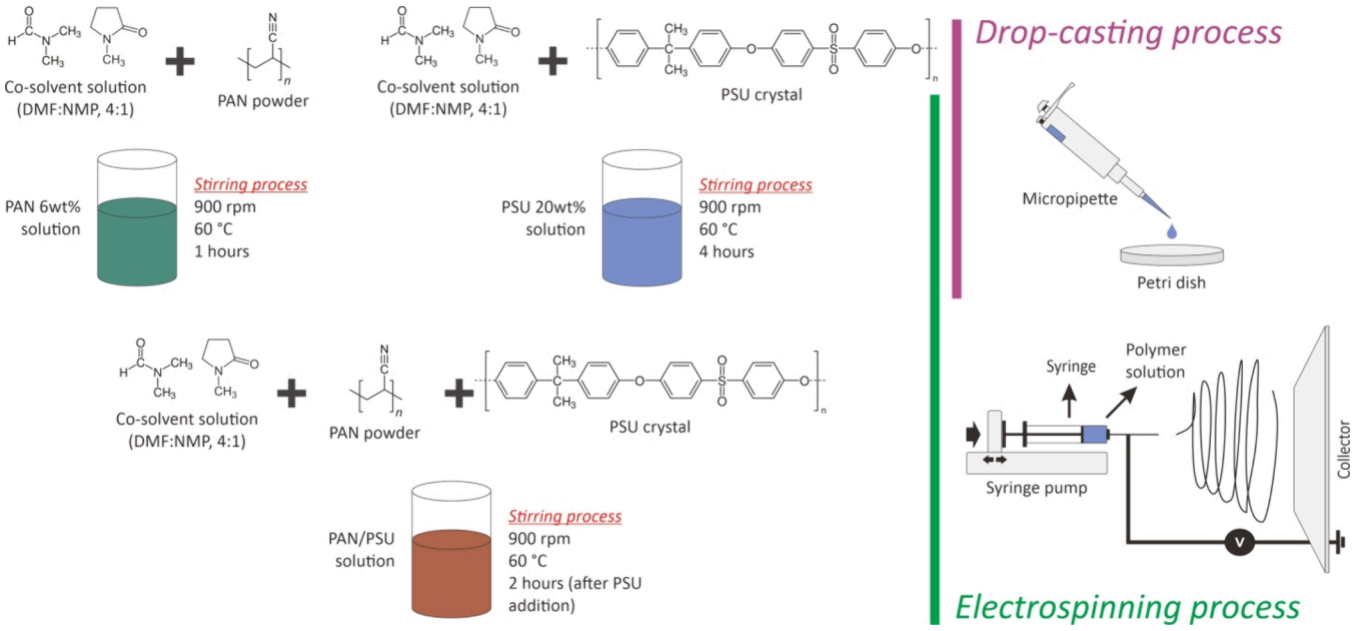

Figure 1. Fabrication processes of nanofibers and thin films. The synthesis processes of polyacrylonitrile (PAN), polysulfone (PSU), and polysulfone-blended polyacrylonitrile (PAN/PSU) solutions were carried out at a temperature of 60 °C and a rotation speed of 900 rpm with different times according to the homogeneity of the solution. The electrospinning method was used to produce nanofibers from PAN, PSU, and PAN/PSU solutions, while the drop-casting method was used to produce PAN and PSU thin films.

straightforward fabrication, and high flexibility in structure/surface modification.[26−30] Moreover, typical diameters of electrospun PAN nanofibers are smaller than 500 nm,[31] leading to their potential to have good air permeability and high filtration efficiency for particles of <1 μm. Nonetheless, all those advantageous properties also come with a drawback, where unmodified or as-prepared PAN nanofibers typically possess hydrophilic surface characteristics.[32,33] Thus, several attempts have been made to increase their hydrophobicity levels, which are mainly by modifying or coating their surfaces (e.g., using fluoroamine compounds,[34] polytetrafluoroethylene (PTFE),[35,36] and nanoparticle-doped polystyrene (PS)), performing carbonization, and aligning their direction without any additional surface treatment (e.g., extruding a PAN solution through an anodic alumina template into a solidifying solution).[37] Although those approaches have successfully demonstrated water contact angle (WCA) enhancements, and the fabricated PAN nanofiber surfaces have been able to be transformed from hydrophilic to hydrophobic or even superhydrophobic characteristics, they still face several challenges. First, fluoroamine and PTFE are among the listed materials of per- and polyfluoroalkyl substances (PFAS), which are a class of fluorinated organic chemicals considered as contaminants of emerging concern produced by various industries.[38] These PFAS have been the focus of many regulatory initiatives across Asia, the European Union (EU), and the USA, where their use may be restricted in the near future.[39,40] Second, besides adding more processing cost and complexity, the carbonization process will result in more brittle carbonized PAN nanofibers, lowering their robustness during the air filtration process. Such nanofibers usually fail under mechanical load at critical flaws.[41,42] Lastly, the homogeneity of the aligned PAN nanofibers yielded by anodic alumina template-based extrusion is difficult to control.[37] Therefore, the materials science research communities keep looking for other alternative strategies to enhance the surface hydrophobicity of PAN nanofibers effectively.

In this work, a low-cost yet effective strategy to produce superhydrophobic composite nanofiber membranes is proposed, employing PAN and polysulfone (PSU) as base and blending materials, respectively. PSU has been selected as a surface-wetting modifier because of its hydrophobic nature, which allows it to repel water droplets.[43−45] The controllability of morphology and wettability behavior of the PAN/PSU nanofibrous mats having altered mixture ratios was investigated. Moreover, chemical compositions of fabricated PAN nanofibers before and after adding different concentrations of PSU into the solutions were analyzed to validate the presence of PSU in PAN/PSU composite nanofibers. Finally, WCA measurements were conducted to evaluate the hydrophobicity enhancement of the fabricated membranes.

MATERIALS AND METHODS

Reagents and Instruments. Polyacrylonitrile (PAN) powder (Mw 150,000 g·mol^{-1}), polysulfone (PSU) crystals (Mw 22,000 g·mol^{-1}), and *N*,*N*-dimethylformamide (DMF) were all purchased from Sigma-Aldrich, Singapore. The 1-methyl-2-pyrrolidone (NMP) was a product of Merck, Germany. All materials were used without any purification process. The morphologies and chemical compositions of the prepared nanofibers were investigated utilizing scanning electron microscopy (SEM, JEOL JSM-6510) and Fourier-transform infrared spectroscopy (FTIR, Thermo Nicolet iS10). An electrospinning machine (FM-ELS001, Fumalife, Indonesia) was utilized to fabricate the nanofiber membrane. A water contact angle (WCA) test instrument (Fumalife, Indonesia) was employed to investigate the nanofiber membrane wettability characteristics (i.e., WCA levels). ImageJ and Avogadro software were used to measure the diameter of the nanofiber and create a 3D illustration of the chemical structure, respectively.

https://doi.org/10.1021/acsomega.4c03554
ACS Omega 2024, 9, 29840−29847

Nanofiber Fabrication Process. PAN powder of 0.307 g was dissolved into 5 mL of cosolvent solutions (DMF:NMP, 4:1) to obtain PAN solutions with a concentration of 6 wt %. The materials were put into a 10 mL beaker glass and then stirred using a hot plate stirrer with a rotation speed of 900 rpm and a temperature of 60 °C for 1 h. After the 6 wt % PAN solutions had been homogeneous, PSU crystals were added with various concentrations of 0.5, 1, 1.5, and 2 wt % to them, which are denoted as PAN/PSU.V1, PAN/PSU.V2, PAN/PSU.V3, and PAN/PSU.V4, respectively. The PAN/PSU composite solutions were stirred with a rotation speed of 900 rpm and a temperature of 60 °C for 2 h. In addition to PAN and PAN/PSU nanofibers, PSU nanofibers were also fabricated. PSU crystals of 1.181 g were dissolved into 5 mL of cosolvent solutions (DMF:NMP, 4:1) by a stirring process using a hot plate stirrer with a rotation speed of 900 rpm and a temperature of 60 °C for 4 h to obtain 20 wt % PSU solutions. The concentrations of PAN and PSU in this research refer to the reports of previous studies.[46,47]

The solutions from the synthesis processes were put into a 10 cc·mL^{-1} syringe with a 25 G × 1″ needle. The syringe was then placed into the electrospinning machine for the nanofiber fabrication process, where the needle was used as the positive pole while the ground was connected to the plate collector. The parameters used in the electrospinning machine were a voltage of 10 kV and a tip-to-collector distance of 15 cm. The electrospinning process was carried out at an ambient temperature of (29.4 ± 0.1) °C. This temperature range was measured using a temperature sensor of SHT31 from Sensirion AG, Switzerland, during the nanofiber fabrication process. The illustration of the nanofiber fabrication process can be seen in Figure 1.

Thin Film Fabrication Process. PAN, PSU, and PAN/PSU thin films were provided in the study for comparison purposes with the nanofiber samples. The thin films were prepared using the drop-casting method, where the used solutions were 6 wt % PAN, 6 wt % PAN with PSU blended in various concentrations (i.e., 0.5, 1, 1.5, and 2 wt %) and 20 wt % PSU with the same synthesis process as the previous section (i.e., the nanofiber fabrication process). All solutions were dropped as much as 100 μL on a Petri dish using a micropipette and dried overnight to obtain PAN and PSU thin films (see Figure 1).

RESULTS AND DISCUSSION

Morphology and Size Analysis of Nanofibers. After synthesizing all the samples (i.e., PAN, PAN/PSU, and PSU nanofiber membranes, and PAN and PSU thin films), their morphologies were investigated using SEM, especially for the PAN and PAN/PSU nanofibers, to evaluate the possible structural modifications on surfaces and diameters of PAN nanofibers affected by the PSU additions (see Figure 2). PAN nanofibers have a smooth and continuous structure, as in the previous report[48] (see Figure 2a). After adding PSU with various concentrations (0.5, 1, 1.5, and 2 wt %, denoted as PAN/PSU.V1, PAN/PSU.V2, PAN/PSU.V3, and PAN/PSU.V4) on PAN nanofibers, the fabricated composite nanofibers do not undergo significant changes in their morphologies (see Figure 2b). Here, all the PAN/PSU nanofiber variants remain in similar sizes, and their continuity can be kept smooth during the electrospinning process. In addition to PAN and PAN/PSU nanofibers, SEM images of PSU nanofibers are also provided in Figure 2c. PSU nanofibers

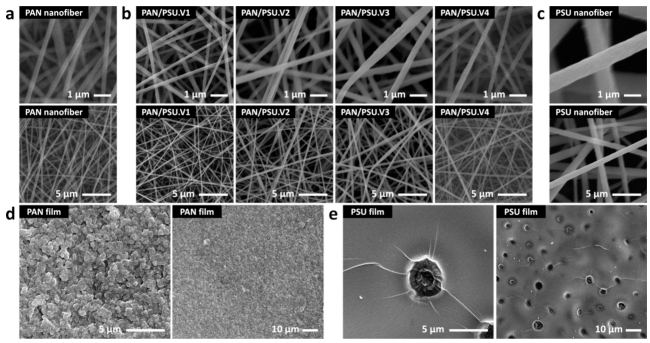

Figure 2. Scanning electron microscopy (SEM) images of various nanofibers (PAN, PSU, and PAN/PSU) and thin films (PAN and PSU). (a) PAN nanofibers. (b) Four different PAN/PSU composite nanofibers (i.e., PAN/PSU.V1, PAN/PSU.V2, PAN/PSU.V3, and PAN/PSU.V4 nanofibers) resulting from additions of PSU concentration of 0.5, 1, 1.5, and 2 wt %, respectively. (c) PSU nanofibers. The first and second rows of the nanofiber images were taken at magnifications of 15,000× and 5,000× , respectively. Thin films made of (d) PAN and (e) PSU. The thin film images were taken at (d) 5,000× and (e) 1,000× magnification levels.

have almost the same morphology as PAN and PAN/PSU nanofibers (i.e., smooth and continuous). However, they possess a much larger diameter. Figure 2 panels d and e show the SEM images of the PAN and PSU thin films. The PAN thin film looks to have a rough morphology. Meanwhile, the PSU thin film appears to have a smoother and flatter texture with some pores on its surface.

Furthermore, to determine nanofiber diameter size distributions, the acquired SEM images of PAN, PAN/PSU, and PSU nanofibers were processed and analyzed using ImageJ software (see Figure 3a–f). Based on the measurement results, the diameter of the PAN nanofibers is (308 ± 43) nm (see Figure 3a). Only a slight fiber size change was found in PAN/PSU nanofibers, where the composite nanofiber variants of PAN/PSU.V1, PAN/PSU.V2, PAN/PSU.V3, and PAN/PSU.V4 possessed diameters of (222 ± 32), (301 ± 63), (392 ± 79), and (290 ± 60) nm, respectively (see Figure 3b–e). Considering the standard deviations measured from those fibers, it is indicated that although the PSU concentration has been changed, it does not influence the structure and size of the nanofibers significantly, and it also indicates that their continuity can be maintained. All four composite membranes (PAN/PSU.V1–PAN/PSU.V4) still possessed an average diameter of (301 ± 70) nm. Figure 3f shows the size distribution of PSU nanofibers, which indicates a larger diameter of (917 ± 214) nm. The high standard deviation value of the measurement indicates that the PSU nanofiber has shortcomings in maintaining size uniformity. For filtration membranes, a smaller nanofiber diameter is more advantageous.[49,50] Thus, PAN/PSU nanofibers provide more desirable characteristics than PSU nanofibers. Moreover, according to SEM images of all fabricated nanofibers, PAN/PSU nanofibers have a smooth morphology and good continuity for all variations. Differences in nanofiber size distribution are depicted in Figure 3g. Nonetheless, again, the nanofiber diameter can be tuned by adjusting the electrospinning parameters (e.g., collector speed solid continual cylinder, working voltage, and tip-to-collector distance).

Chemical Analysis of Nanofibers. After confirming the structural characteristics of the PAN and PAN/PSU composite

https://doi.org/10.1021/acsomega.4c03554
ACS Omega 2024, 9, 29840−29847

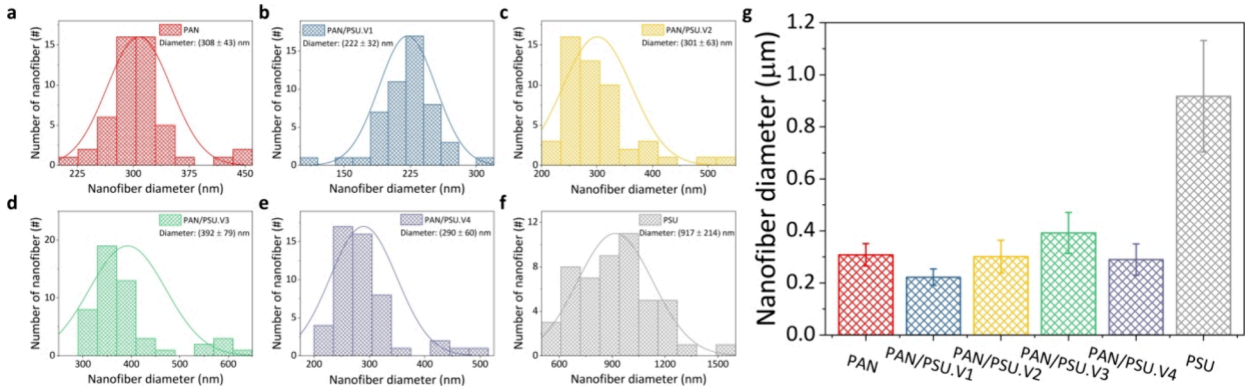

Figure 3. Size distributions of PAN, PSU, and PAN/PSU nanofiber membranes. Measured size distributions of (a) PAN, (b) PAN/PSU.V1, (c) PAN/PSU.V2, (d) PAN/PSU.V3, (e) PAN/PSU.V4, and (f) PSU nanofibers. (g) Evaluation of the measured diameters of different nanofibers. The nanofiber diameters were determined using ImageJ based on the SEM images shown in Figure 2.

nanofibers using SEM, we performed FTIR spectroscopy to analyze their chemical compositions (see Figure 4). In addition, an additional sample of bare PSU crystals was also prepared and characterized to ensure that the characteristics of PSU additions could be seen in the PAN/PSU composite nanofibers.

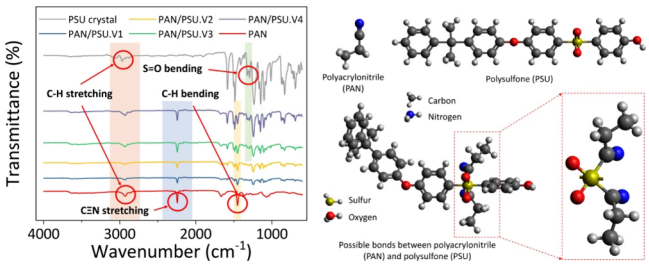

Figure 4. Fourier-transform infrared (FTIR) spectra and illustration of possible bonding of the prepared PAN/PSU composite nanofibers. In addition to four PAN/PSU nanofiber variants (i.e., PAN/PSU.V1, PAN/PSU.V2, PAN/PSU.V3, and PAN/PSU.V4 nanofibers), both bare PAN nanofibers and PSU crystals were also characterized in terms of their FTIR spectra. A single covalent bond (σ bond) occurs in PAN/PSU composite nanofibers.

For the PAN nanofibers, two characteristic peaks at 2924 and 2243 cm^{-1} were observed, indicating the presence of C−H and C≡N stretching, respectively.[51] Besides them, a C−H bending peak was also seen at 1452 cm^{-1}.[52] Meanwhile, for the PSU crystals, although a C−H stretching peak was also observed at 2925 cm^{-1},[53,54] similar to that of PAN nanofibers, a different characteristic peak at 1321 cm^{-1} was found, indicating S═O bending.[55]

Considering those peaks at bare PAN nanofibers and bare PSU crystals, the appearing characteristic peaks of PAN/PSU nanofibers were expected to be a combination of peaks from both bare PAN nanofibers and bare PSU crystals. Indeed, they have been evident from the presence of C−H and C≡N stretching peaks at 2926 and 2243 cm^{-1}, respectively. In addition, the effect of PSU addition on the PAN/PSU nanofibers was also observed in the S═O bending peak at 1322 cm^{-1}, which did not appear in the PAN nanofibers (see Figure 4). This S═O bending peak became higher when the PSU concentration was increased. Hence, the strongest FTIR spectroscopy signal was depicted by the PAN/PSU.V4 sample with a PSU concentration of 2 wt %.

In the PAN/PSU composite, the reaction possibly comes from the carbon atom (C) in the nitrile group (−CN) of PAN and engages in a nucleophilic attack on the sulfur atom (S) in the sulfonyl group (SO_2) of PSU.[56,57] This process is predicted to break the carbon−nitrogen bonds in the nitrile group and the sulfur−oxygen bonds in the sulfonyl group. This reaction leads to a new covalent bond, with the copolymer exhibiting a chemical structure that integrates repeating units from PAN and PSU. The specific type of bond formed is expected to be a single covalent bond (σ bond) (see Figure 4).

Water Contact Angle Analysis. The final assessment carried out for the fabricated nanofibers (i.e., PAN, PAN/PSU, and PSU nanofibers) and thin films (i.e., PAN, PAN/PSU, and PSU thin films) was WCA analysis. This WCA characterization is a widely used test to determine the level of hydrophilicity and hydrophobicity of a coating or material.[58] WCA measurements were performed three times (n = 3), where the standard deviation (SD) value was used as the error value. Figure 5a shows the result of the WCA analysis of PAN nanofiber. It is obvious that prior to any blending treatment, the PAN nanofiber surface has hydrophilic properties with a WCA value of (14 ± 1)°. A similar WCA value was obtained by the PAN thin film, which is (13 ± 1)° (see Figure 5b). After the addition of PSU, the WCA values of the composite nanofibers increased significantly up to (156 ± 6)°, (160 ± 4)°, (156 ± 6)°, and (158 ± 4)° for PAN/PSU.V1, PAN/PSU.V2, PAN/PSU.V3, and PAN/PSU.V4 nanofibers, respectively (see Figure 5c). The increase in WCA occurs because the nanofibers obtained an additional property from PSU, which is hydrophobic. Here, the bare PSU nanofibers possess a WCA of (163 ± 2)° (see Figure 5d). Interestingly, the wettability conversion from a hydrophilic surface (WCA ∼ 14°) in bare PAN condition to a superhydrophobic surface (WCA > 150°) in PAN/PSU composite structures could be obtained even at the lowest tested PSU concentration of 0.5 wt %.

In such nanofibrous mats, two essential features are typically responsible for the obtained superhydrophobicity (high WCA), which are the low surface energy and rough surface morphology (surface roughness/smoothness) of the fiber surfaces.[59−61] Here, unblended PAN nanofibers exhibited poor hydrophobicity because of their polar functional groups (e.g., amide linkage and hydroxyl groups in the PAN chains).[60] From SEM images in Figure 2, their morphology and surface are smooth without any bead structures. Thus, surface

https://doi.org/10.1021/acsomega.4c03554
ACS Omega 2024, 9, 29840−29847

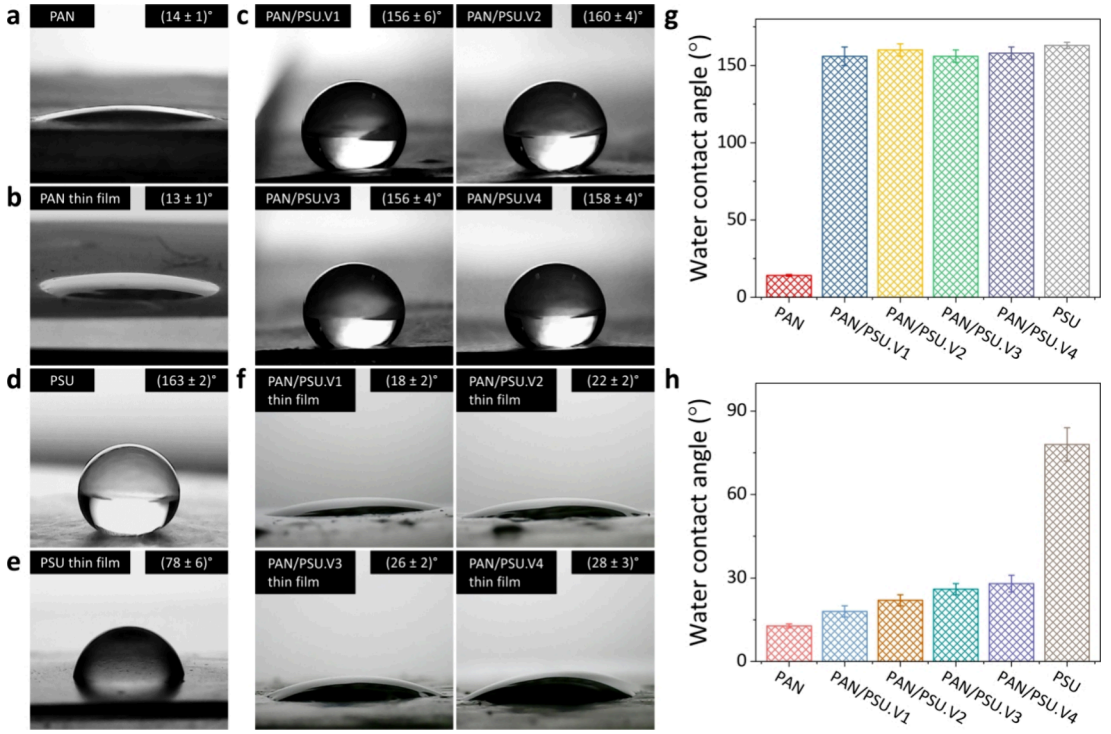

Figure 5. Water contact angle (WCA) analysis of the nanofibers (PAN, PSU, and PAN/PSU) and thin films (PAN, PAN/PSU, and PSU). (a) PAN nanofiber and (b) PAN thin film have a low WCA of <14.2°, indicating their hydrophilic properties. (c) After the addition of PSU to the nanofiber (i.e., PAN/PSU.V1, PAN/PSU.V2, PAN/PSU.V3, and PAN/PSU.V4), the nanofiber experiences an increase in WCA until it reaches the superhydrophobic level (>156°). (d) PSU nanofiber has superhydrophobic characteristics. (e) PSU thin film shows a low WCA, indicating the superiority of the nanofiber structure compared to the thin film. (f) WCA of PAN/PSU thin film (<28°). A summary of the measured WCA values for all fabricated (g) nanofibers and (h) thin films.

roughness improvement of the PAN material was simply coming from its modification from planar to 3D nanofiber structures. It has been known that the hydrophobicity of solid surfaces can be enhanced by physically increasing their roughness (e.g., creating 3D nanostructures like nanoparticles, nanofibers, nanorods, or nanopillars[62−65]), so that the air can be trapped inside the nanoscopic surface textures. This has been proven in the WCA result comparison between the nanofiber and thin film forms of both PAN and PSU, where the nanofiber yields higher WCA (see Figure 5a,b and Figure 5d,e). In addition, this phenomenon can also be found in PAN/PSU thin films, which have a WCA of <28°. A summary of the measured WCA values for various nanofiber and thin film samples can be seen in Figure 5g,h, respectively.

In the case of the PAN/PSU nanofiber, the fraction of liquid−solid contact can be dramatically decreased, yielding high liquid repellency.[66,67] Nonetheless, in reality, when the nanofiber membranes are used as particle filters, they can potentially be exposed to harsh environments (e.g., raining storms). Here, the water pressure influenced by the external factors (e.g., droplet impact) can be greater than the critical pressure at the air−liquid interface, resulting in a transition from the Cassie−Baxter nonwetting state to the Wenzel wetting state, where water is steeped into the surface textures and cannot overcome the energy barrier to return to the nonwetting state.[68,69]

Again, besides morphology enhancement, surface chemistry modification by PSU dopants plays a critical role in the resulting superhydrophobicity of PAN/PSU composite nanofibers since it changes their surface energy. As we did not do any further treatment of the received PSU (see Materials and Methods section), the original nature of hydrophobicity affecting low surface energy of PSU can be kept in the PAN/PSU mixture solution before and after electrospinning. It should be mentioned that, in other studies, the hydrophobicity of such PSU can be converted to hydrophilicity, e.g., by oxygen plasma[70] and bovine serum albumin (BSA) solution[71] treatments. However, in our case, these additional treatments are not required, keeping the low-cost preparation process of the PAN/PSU composite nanofiber membranes. Moreover, PSU is a nonpolar active group, which has a low affinity for water. Low affinity for water makes it very difficult for PSU to interact with water. When PSU is mixed into PAN, and a composite solution is formed, the nature of PSU, which has a low affinity for water, makes the composite solution have the same properties. Thus, PAN/PSU also has a high level of hydrophobicity (based on WCA in Figure 5).

■ CONCLUSIONS

Superhydrophobic polysulfone-blended polyacrylonitrile (PAN/PSU) composite nanofiber membranes have been fabricated in this study using an electrospinning technique. Scanning electron microscopy (SEM) results determine that the bare PAN nanofibers have a smooth and continuous structure with a diameter of (308 ± 43) nm and do not undergo significant changes in morphology and size after adding PSU. Fourier-transform infrared (FTIR) spectra show a change in chemical composition after the addition of PSU; the absorption peaks of the PAN/PSU nanofibers were observed, as found in both the spectra of PAN nanofibers and PSU crystals, indicating that the blending process of these two polymers was successful. The hydrophobicity of the nanofibers,

https://doi.org/10.1021/acsomega.4c03554
ACS Omega 2024, 9, 29840−29847

an important property concerning air filtration performance, was determined based on the analysis of the water contact angle (WCA). The PAN/PSU composite nanofibers can yield a WCA value of >156°, demonstrating their superhydrophobic characteristics, which are similar to that of PSU nanofibers (i.e., (163 ± 2)°). Therefore, the fabricated nanofibers are expected to have high potential to be applied as an air filtration membrane. However, the particle filtration performance of the PAN/PSU nanofiber membranes still needs to be evaluated in the next study to validate their practical applications. Moreover, the currently fabricated membranes are still limited to the use of a standard lab-scale needle-based electrospinning, which cannot implement a typical industrial-scale roll-to-roll electrospinning process. Thus, the employed PAN and PSU concentrations, as well as other processing recipe parameters shown in this study, require adjustment when this polymer blending strategy is transferred to industry to unlock its full high potential for manufacturing real membrane products.

AUTHOR INFORMATION

Corresponding Author

Kuwat Triyana − *Department of Physics, Faculty of Mathematics and Natural Sciences, Universitas Gadjah Mada, Yogyakarta 55281, Indonesia;* orcid.org/0000-0002-1466-4364; Email: triyana@ugm.ac.id

Authors

Rizky Aflaha − *Department of Physics, Faculty of Mathematics and Natural Sciences, Universitas Gadjah Mada, Yogyakarta 55281, Indonesia;* orcid.org/0000-0001-6039-5751

Linda Ardita Putri − *Department of Physics, Faculty of Mathematics and Natural Sciences, Universitas Gadjah Mada, Yogyakarta 55281, Indonesia*

Chlara Naren Maharani − *Department of Physics Education, Faculty of Mathematics and Natural Sciences, Universitas Negeri Yogyakarta, Yogyakarta 55281, Indonesia*

Aditya Rianjanu − *Department of Materials Engineering and Center for Green and Sustainable Materials, Institut Teknologi Sumatera, Way Hui, Jati Agung, Lampung 35365, Indonesia;* orcid.org/0000-0001-7852-3619

Roto Roto − *Department of Chemistry, Faculty of Mathematics and Natural Sciences, Universitas Gadjah Mada, Yogyakarta 55281, Indonesia;* orcid.org/0000-0001-8163-4651

Hutomo Suryo Wasisto − *PT Nanosense Instrument Indonesia, Yogyakarta 55167, Indonesia;* orcid.org/0000-0002-4522-3625

Complete contact information is available at: https://pubs.acs.org/10.1021/acsomega.4c03554

Author Contributions

R.A.: conceptualization; investigation; visualization; formal analysis; writing-original draft; writing-review and editing. **L.A.P.** and **C.N.M.:** investigation. **A.R.** and **R.R.:** formal analysis; writing-review and editing. **H.S.W.:** validation; formal analysis; funding acquisition; writing-original draft; writing-review and editing. **K.T.:** conceptualization; resources; funding acquisition; supervision; formal analysis; writing-review and editing. All authors approved the final manuscript.

Notes

The authors declare no competing financial interest.

ACKNOWLEDGMENTS

The authors thank all PT Nanosense Instrument Indonesia and PT Fumalife Sinergi Inovasi employees who have provided technical support in this presented research work.

REFERENCES

(1) Liao, M.; Jian, X.; Zhao, Y.; Fu, X.; Wan, M.; Zheng, W.; et al. Sandwich-like" structure electrostatic spun micro/nanofiber polylactic acid-polyvinyl alcohol-polylactic acid film dressing with metformin hydrochloride and puerarin for enhanced diabetic wound healing. *Int. J. Biol. Macromol.* **2023**, *253*, No. 127223.

(2) Gao, S.; Xiong, X.; Xie, H.; zha, X.; Li, P.; Kong, F.; et al. Periplaneta americana extract incorporated silk fibroin nanofiber mat: A potential antioxidant dressing for wound healing. *Process Biochem* **2023**, *134*, 218−31.

(3) Zhu, J.; Yan, C.; Li, G.; Cheng, H.; Li, Y.; Liu, T.; et al. Recent developments of electrospun nanofibers for electrochemical energy storage and conversion. *Energy Storage Mater.* **2024**, *65*, No. 103111.

(4) Wang, J.; Xin, Z.; Wang, Y.; Hao, H.; Liu, S.; Wang, Q.; et al. Reinforced energy storage performance of poly(vinylidene fluoride) composite films by filling with surface fluorinated one-dimensional barium titanate nanofibers. *J. Alloys Compd.* **2023**, *966*, No. 171601.

(5) Rianjanu, A.; Rayhan, M. A. A. P.; Aulya, M.; Aflaha, R.; Triyana, K.; Taher, T.; Wasisto, H. S.; et al. Early Spoilage Detection of Cultured Pacific White Shrimp Using Quartz Crystal Microbalance Gas Sensors. *ChemistrySelect* **2024**, *9*, No. e202304694.

(6) Wang, D.; Zhang, D.; Li, P.; Yang, Z.; Mi, Q.; Yu, L. Electrospinning of Flexible Poly(vinyl alcohol)/MXene Nanofiber-Based Humidity Sensor Self-Powered by Monolayer Molybdenum Diselenide Piezoelectric Nanogenerator. *Nano-Micro Lett.* **2021**, *13*, 57.

(7) Wang, D.; Zhang, D.; Guo, J.; Hu, Y.; Yang, Y.; Sun, T.; et al. Multifunctional poly(vinyl alcohol)/Ag nanofibers-based triboelectric nanogenerator for self-powered MXene/tungsten oxide nanohybrid NO2 gas sensor. *Nano Energy* **2021**, *89*, No. 106410.

(8) Wang, J.; Zhang, D.; Gao, Y.; Chen, F.; Wang, T.; Xia, H.; et al. Fast-response hydrogen sulfide gas sensor based on electrospinning Co3O4 nanofibers-modified CuO nanoflowers: Experimental and DFT calculation. *Sensors Actuators B Chem.* **2023**, *396*, No. 134579.

(9) Aflaha, R.; Sari, N. L. I.; Katriani, L.; As'ari, A. H.; Kusumaatmaja, A.; Rianjanu, A.; et al. Maltodextrin-overlaid polyvinyl acetate nanofibers for highly sensitive and selective room-temperature ammonia sensors. *Microchem J.* **2023**, *193*, No. 109237.

(10) Aflaha, R.; Katriani, L.; As'ari, A. H.; Sari, N. L. I.; Kusumaatmaja, A.; Rianjanu, A.; et al. Enhanced trimethylamine gas sensor sensitivity based on quartz crystal microbalance using nanofibers overlaid with maltodextrin. *MRS Commun.* **2023**, *13*, 664−72.

(11) Roto, R.; Rianjanu, A.; Fatyadi, I. A.; Kusumaatmaja, A.; Triyana, K. Enhanced sensitivity and selectivity of ammonia sensing by QCM modified with boric acid-doped PVAc nanofiber. *Sensors Actuators, A Phys.* **2020**, *304*, No. 111902.

(12) Aminu, N.; Ilyasu, S.; Al-Kassim Hassan, M.; Kurfi, F. S.; Jatau, A. I.; Chan, S.-Y.; et al. Applications of nanofibers drug delivery system in cancer therapy. *J. Drug Deliv Sci. Technol.* **2023**, *90*, No. 105128.

(13) Chen, Y.; Wang, N.; Jensen, M.; Li, X. Low-temperature welded PAN/TPU composite nanofiber membranes for water filtration. *J. Water Process Eng.* **2022**, *47*, No. 102806.

(14) Lu, T.; Cui, J.; Qu, Q.; Wang, Y.; Zhang, J.; Xiong, R.; et al. Multistructured Electrospun Nanofibers for Air Filtration: A Review. *ACS Appl. Mater. Interfaces* **2021**, *13*, 23293−313.

(15) Sundarrajan, S.; Tan, K. L.; Lim, S. H.; Ramakrishna, S. Electrospun Nanofibers for Air Filtration Applications. *Procedia Eng.* **2014**, *75*, 159−63.

(16) De Riccardis, M. F. Electrospun Nanofibrous Membranes for Air Filtration: A Critical Review. *Compounds* **2023**, *3*, 390−410.

(17) Su, Q.; Wei, Z.; Zhu, C.; Wang, X.; Zeng, W.; Wang, S.; et al. Multilevel structured PASS nanofiber filter with outstanding thermal stability and excellent mechanical property for high-efficiency particulate matter removal. *J. Hazard Mater.* **2022**, *431*, No. 128514.
(18) Yu, X.; Li, C.; Tian, H.; Yuan, L.; Xiang, A.; Li, J.; et al. Hydrophobic cross-linked zein-based nanofibers with efficient air filtration and improved moisture stability. *Chem. Eng. J.* **2020**, *396*, No. 125373.
(19) Liu, H.; Huang, J.; Mao, J.; Chen, Z.; Chen, G.; Lai, Y. Transparent Antibacterial Nanofiber Air Filters with Highly Efficient Moisture Resistance for Sustainable Particulate Matter Capture. *IScience* **2019**, *19*, 214−23.
(20) Liu, T.; Cai, C.; Ma, R.; Deng, Y.; Tu, L.; Fan, Y.; et al. Superhydrophobic Cellulose Nanofiber Air Filter with Highly Efficient Filtration and Humidity Resistance. *ACS Appl. Mater. Interfaces* **2021**, *13*, 24032−41.
(21) Alghoraibi, I, Alomari, S. Different Methods for Nanofiber Design and Fabrication. In *BT - Handbook of Nanofibers*; Barhoum, A., Bechelany, M., Makhlouf, A., Eds.; Springer International Publishing: Cham; 2018; pp 1−46, DOI: 10.1007/978-3-319-42789-8_11-2.
(22) Haider, A.; Haider, S.; Kang, I.-K. A comprehensive review summarizing the effect of electrospinning parameters and potential applications of nanofibers in biomedical and biotechnology. *Arab J. Chem.* **2018**, *11*, 1165−88.
(23) Huang, Y.; Song, J.; Yang, C.; Long, Y.; Wu, H. Scalable manufacturing and applications of nanofibers. *Mater. Today* **2019**, *28*, 98−113.
(24) Xu, J.; Liu, C.; Hsu, P.-C.; Liu, K.; Zhang, R.; Liu, Y.; et al. Roll-to-Roll Transfer of Electrospun Nanofiber Film for High-Efficiency Transparent Air Filter. *Nano Lett.* **2016**, *16*, 1270−5.
(25) Wang, X.; Pellerin, C.; Bazuin, C. G. Enhancing the Electrospinnability of Low Molecular Weight Polymers Using Small Effective Cross-Linkers. *Macromolecules* **2016**, *49*, 891−9.
(26) Hidayat, S. N.; Julian, T.; Rianjanu, A.; Kusumaatmadja, A.; Triyana, K. Quartz crystal microbalance coated by PAN nanofibers and PEDOT:PSS for humidity sensor. *2017 Int Semin Sensors, Instrumentation, Measurement and Metrology (ISSIMM)* **2017**, 119−123.
(27) Cheng, X.; Zhao, L.; Zhang, Z.; Deng, C.; Li, C.; Du, Y.; et al. Highly efficient, low-resistant, well-ordered PAN nanofiber membranes for air filtration. *Colloids Surfaces A Physicochem Eng. Asp* **2022**, *655*, No. 130302.
(28) Kang, Y.; Chen, J.; Feng, S.; Zhou, H.; Zhou, F.; Low, Z.-X.; et al. Efficient removal of high-temperature particulate matters via a heat resistant and flame retardant thermally-oxidized PAN/PVP/SnO2 nanofiber membrane. *J. Membr. Sci.* **2022**, *662*, No. 120985.
(29) Nataraj, S. K.; Yang, K. S.; Aminabhavi, T. M. Polyacrylonitrile-based nanofibers—A state-of-the-art review. *Prog. Polym. Sci.* **2012**, *37*, 487−513.
(30) Ahn, H.; Yeo, S. Y.; Lee, B.-S. Designing Materials and Processes for Strong Polyacrylonitrile Precursor Fibers. *Polymers (Basel)* **2021**, *13*, 2863.
(31) Huang, L.; Song, F.; Ding, H.; Wang, Y.; Zhu, W. Hydrophobic polyacrylonitrile/pitch electrospun nanofibers for oil spill cleanup: Fabrication, optimization, and kinetic investigations. *J. Water Process Eng.* **2022**, *50*, No. 103210.
(32) Pervez, M. N.; Talukder, M. E.; Mishu, M. R.; Buonerba, A.; del Gaudio, P.; Stylios, G. K.; et al. Fabrication of polyethersulfone/polyacrylonitrile electrospun nanofiber membrane for food industry wastewater treatment. *J. Water Process Eng.* **2022**, *47*, No. 102838.
(33) Meng, H.; Cheng, Q.; Li, C. Polyacrylonitrile-based zwitterionic ultrafiltration membrane with improved anti-protein-fouling capacity. *Appl. Surf. Sci.* **2014**, *303*, 399−405.
(34) Almasian, A.; Chizari Fard, G.; Mirjalili, M.; Parvinzadeh Gashti, M. Fluorinated-PAN nanofibers: Preparation, optimization, characterization and fog harvesting property. *J. Ind. Eng. Chem.* **2018**, *62*, 146−55.
(35) Salahuddin, M.; Uddin, M. N.; Hwang, G.; Asmatulu, R. Superhydrophobic PAN nanofibers for gas diffusion layers of proton exchange membrane fuel cells for cathodic water management. *Int. J. Hydrogen Energy* **2018**, *43*, 11530−8.
(36) Wang, D.; Zhang, D.; Yang, Y.; Mi, Q.; Zhang, J.; Yu, L. Multifunctional Latex/Polytetrafluoroethylene-Based Triboelectric Nanogenerator for Self-Powered Organ-like MXene/Metal−Organic Framework-Derived CuO Nanohybrid Ammonia Sensor. *ACS Nano* **2021**, *15*, 2911−9.
(37) Feng, L.; Li, S.; Li, H.; Zhai, J.; Song, Y.; Jiang, L.; et al. Super-Hydrophobic Surface of Aligned Polyacrylonitrile Nanofibers. *Angew. Chemie Int. Ed* **2002**, *41*, 1221−3.
(38) Singh, K.; Kumar, N.; Kumar Yadav, A.; Singh, R.; Kumar, K. Per-and polyfluoroalkyl substances (PFAS) as a health hazard: Current state of knowledge and strategies in environmental settings across Asia and future perspectives. *Chem. Eng. J.* **2023**, *475*, No. 145064.
(39) Brennan, N. M.; Evans, A. T.; Fritz, M. K.; Peak, S. A.; von Holst, H. E. Trends in the Regulation of Per- and Polyfluoroalkyl Substances (PFAS): A Scoping Review. *Int. J. Environ. Res. Public Health* **2021**, *18*, 10900.
(40) Bock, A. R., Laird, B. E. PFAS Regulations: Past and Present and Their Impact on Fluoropolymers. In *Perfluoroalkyl Subst.*; Améduri, B, Ed.; The Royal Society of Chemistry; 2022; pp 1−21 DOI: 10.1039/9781839167591-00001.
(41) Fitzer, E. Pan-based carbon fibers—present state and trend of the technology from the viewpoint of possibilities and limits to influence and to control the fiber properties by the process parameters. *Carbon N Y* **1989**, *27*, 621−45.
(42) Zussman, E.; Chen, X.; Ding, W.; Calabri, L.; Dikin, D. A.; Quintana, J. P.; et al. Mechanical and structural characterization of electrospun PAN-derived carbon nanofibers. *Carbon N Y* **2005**, *43*, 2175−85.
(43) Lutz, H. Ultrafiltration: Fundamentals and Engineering. In *Comprehensive Membrane Science and Engineering*; Drioli, E., Giorno, L., Eds.; Elsevier: Oxford, 2010; pp 115−139, DOI: 10.1016/B978-0-08-093250-7.00037-2.
(44) Yuan, X.; Zhang, Y.; Dong, C.; Sheng, J. Morphology of ultrafine polysulfone fibers prepared by electrospinning. *Polym. Int.* **2004**, *53*, 1704−10.
(45) Wan, H.; Wang, N.; Yang, J.; Si, Y.; Chen, K.; Ding, B.; et al. Hierarchically structured polysulfone/titania fibrous membranes with enhanced air filtration performance. *J. Colloid Interface Sci.* **2014**, *417*, 18−26.
(46) Obaid, M.; Barakat, N. A. M.; Fadali, O. A.; Motlak, M.; Almajid, A. A.; Khalil, K. A. Effective and reusable oil/water separation membranes based on modified polysulfone electrospun nanofiber mats. *Chem. Eng. J.* **2015**, *259*, 449−56.
(47) Rianjanu, A.; Aulya, M.; Rayhan, M. A. A. P.; Aflaha, R.; Maulana, S.; Taher, T.; Sipahutar, W. S.; Maulana, M. I.; Yulianto, N.; Triyana, K.; Wasisto, H. S. Impact of hydrophilic bamboo cellulose functionalization on electrospun polyacrylonitrile nanofiber-based humidity sensors. *MRS Commun.* **2023**, *13*, 514−519.
(48) Rianjanu, A.; Roto, R.; Julian, T.; Hidayat, S. N.; Kusumaatmaja, A.; Suyono, E. A. Polyacrylonitrile Nanofiber-Based Quartz Crystal Microbalance for Sensitive Detection of Safrole. *Sensors* **2018**, *18*, 1150.
(49) Russo, F.; Castro-Muñoz, R.; Santoro, S.; Galiano, F.; Figoli, A. A review on electrospun membranes for potential air filtration application. *J. Environ. Chem. Eng.* **2022**, *10*, No. 108452.
(50) Zhou, Y.; Liu, Y.; Zhang, M.; Feng, Z.; Yu, D.-G.; Wang, K. Electrospun Nanofiber Membranes for Air Filtration: A Review. *Nanomaterials* **2022**, *12*, 1077.
(51) Hassan, H. M. A.; Alsohaimi, I. H.; El-Aassar, M. R.; El-Hashemy, M. A.; El-Sayed, M. Y.; Alotaibi, N. F.; et al. Electrospun TiO2-GO/PAN-CA nanofiber mats: A novel material for remediation of organic contaminants and nitrophenol reduction. *Environ. Res.* **2023**, *234*, No. 116587.
(52) Özcan, M. Green synthesis of ZnO nanoparticles decorating electrospun PAN nanofibers for enhanced radiation shielding. *Phys. B Condens Matter* **2024**, *674*, No. 415584.

https://doi.org/10.1021/acsomega.4c03554
ACS Omega 2024, 9, 29840−29847

(53) Filimon, A.; Albu, R. M.; Stoica, I.; Avram, E. Blends based on ionic polysulfones with improved conformational and microstructural characteristics: Perspectives for biomedical applications. *Compos Part B Eng.* **2016**, *93*, 1−11.
(54) Filimon, A.; Stoica, I.; Onofrei, M. D.; Bargan, A.; Dunca, S. Quaternized polysulfones-based blends: Surface properties and performance in life quality and environmental applications. *Polym. Test* **2018**, *71*, 285−95.
(55) Filimon, A.; Olaru, N.; Doroftei, F.; Coroaba, A.; Dunca, S. Processing of quaternized polysulfones solutions as tool in design of electrospun nanofibers: Microstructural characteristics and antimicrobial activity. *J. Mol. Liq.* **2021**, *330*, No. 115664.
(56) Light, K. M.; Yamanaka, Y.; Odaka, M.; Solomon, E. I. Spectroscopic and computational studies of nitrile hydratase: insights into geometric and electronic structure and the mechanism of amide synthesis. *Chem. Sci.* **2015**, *6*, 6280−94.
(57) Nelp, M. T.; Song, Y.; Wysocki, V. H.; Bandarian, V. A Protein-derived Oxygen Is the Source of the Amide Oxygen of Nitrile Hydratases. *J. Biol. Chem.* **2016**, *291*, 7822−9.
(58) Liu, X.; Zhang, D.; Wang, D.; Li, T.; Song, X.; Kang, Z. A humidity sensing and respiratory monitoring system constructed from quartz crystal microbalance sensors based on a chitosan/polypyrrole composite film. *J. Mater. Chem. A* **2021**, *9*, 14524−33.
(59) Du, Q.; Zhou, P.; Pan, Y.; Qu, X.; Liu, L.; Yu, H.; et al. Influence of hydrophobicity and roughness on the wetting and flow resistance of water droplets on solid surface: A many-body dissipative particle dynamics study. *Chem. Eng. Sci.* **2022**, *249*, No. 117327.
(60) Ahmad, A.; Albargi, H.; Ali, M.; Batool, M.; Nazir, A.; Qadir, M. B.; et al. Differential carbonization-shrinkage induced hierarchically rough PAN/PDMS nanofiber composite membrane for robust multimodal superhydrophobic applications. *J. Sci. Adv. Mater. Devices* **2023**, *8*, No. 100536.
(61) Parvate, S.; Dixit, P.; Chattopadhyay, S. Superhydrophobic Surfaces: Insights from Theory and Experiment. *J. Phys. Chem. B* **2020**, *124*, 1323−60.
(62) Yulianto, N.; Refino, A. D.; Syring, A.; Majid, N.; Mariana, S.; Schnell, P.; et al. Wafer-scale transfer route for top−down III-nitride nanowire LED arrays based on the femtosecond laser lift-off technique. *Microsystems Nanoeng* **2021**, *7*, 32.
(63) Refino, A. D.; Adhitama, E.; Bela, M. M.; Sadhujan, S.; Harilal, S.; Eldona, C.; et al. Impact of exposing lithium metal to monocrystalline vertical silicon nanowires for lithium-ion microbatteries. *Commun. Mater.* **2023**, *4*, 58.
(64) Refino, A. D.; Yulianto, N.; Syamsu, I.; Nugroho, A. P.; Hawari, N. H.; Syring, A.; et al. Versatilely tuned vertical silicon nanowire arrays by cryogenic reactive ion etching as a lithium-ion battery anode. *Sci. Rep* **2021**, *11*, No. 19779.
(65) Nuraje, N.; Khan, W. S.; Lei, Y.; Ceylan, M.; Asmatulu, R. Superhydrophobic electrospun nanofibers. *J. Mater. Chem. A* **2013**, *1*, 1929−46.
(66) Checco, A.; Ocko, B. M.; Rahman, A.; Black, C. T.; Tasinkevych, M.; Giacomello, A.; et al. Collapse and Reversibility of the Superhydrophobic State on Nanotextured Surfaces. *Phys. Rev. Lett.* **2014**, *112*, No. 216101.
(67) Wu, G.; Zhao, Y.; Ge, D.; Zhao, Y.; Yang, L.; Yang, S. Highly Robust, Pressure-Resistant Superhydrophobic Coatings from Monolayer Assemblies of Chained Nanoparticles. *Adv. Mater. Interfaces* **2021**, *8*, No. 2000681.
(68) Xiang, Y.; Huang, S.; Lv, P.; Xue, Y.; Su, Q.; Duan, H. Ultimate Stable Underwater Superhydrophobic State. *Phys. Rev. Lett.* **2017**, *119*, No. 134501.
(69) Lafuma, A.; Quéré, D. Superhydrophobic states. *Nat. Mater.* **2003**, *2*, 457−60.
(70) Kim, K. S.; Lee, K. H.; Cho, K.; Park, C. E. Surface modification of polysulfone ultrafiltration membrane by oxygen plasma treatment. *J. Membr. Sci.* **2002**, *199*, 135−45.
(71) Nabe, A.; Staude, E.; Belfort, G. Surface modification of polysulfone ultrafiltration membranes and fouling by BSA solutions. *J. Membr. Sci.* **1997**, *133*, 57−72.

https://doi.org/10.1021/acsomega.4c03554
ACS Omega 2024, 9, 29840−29847